Evidence for an accelerating wind as the broad-line region in NGC 3516

J.B. Hutchings[1], G. A. Kriss[2,3], R. F. Green[4], M. Brotherton[4], M. E. Kaiser[3], A. P. Koratkar[2], W. Zheng[3]

ABSTRACT

Spectroscopic data in wavelengths 900–3000 Å have been obtained in a low flux state of the nucleus of the Seyfert 1 galaxy NGC 3516. The line profiles show P Cygni characteristics, particularly in O VI λ1032, and are compared with data from an earlier higher state. The profiles are suggestive of, and consistent with, an accelerating wind driven by a disk continuum source, in which the ionisation radii have changed. This scenario may apply to the formation of other broad emission lines in AGN.

1. Introduction

While it is now known that roughly 50% of all Seyfert galaxies exhibit UV absorption lines (Crenshaw et al. 1999), the Seyfert 1 galaxy NGC 3516 is unique in that its absorption lines are the strongest and most variable of any object in this class (Koratkar et al. 1996; Goad et al. 1999). The deep, broad C IV absorption first visible in *International Ultraviolet Explorer (IUE)* spectra (Ulrich 1988) is reminiscent of the broad absorption lines seen in $\sim$ 10% of radio-quiet QSOs (Weymann et al. 1991). In many Seyfert 1 galaxies UV-absorbing gas appears in conjunction with X-ray absorption by highly ionized gas. These X-ray "warm absorbers" are equally common in Seyferts (Reynolds 1997; George et al. 1998). Crenshaw et al. (1999) note that all instances of X-ray absorption also exhibit UV absorption. While Mathur et al. (1994; 1995; 1997) have suggested that

[1]Herzberg Insitute of Astrophysics, National Research Council of Canada, Victoria, B.C. V8X 4M6, Canada

[2]Space Telescope Science Institute, 3700 San Martin Drive, Baltimore, MD 21218; gak@stsci.edu

[3]Center for Astrophysical Sciences, Department of Physics and Astronomy, The Johns Hopkins University, Baltimore, MD 21218–2686

[4]Kitt Peak National Observatory, National Optical Astronomy Observatories, P.O. Box 26732, 950 North Cherry Ave., Tucson, AZ, 85726-6732

the same gas gives rise to both the X-ray and UV absorption, the spectral complexity of the UV and X-ray absorbers indicates that a wide range of physical conditions are present. In NGC 3516, the UV absorption in the Lyman lines, O VI, N V, Si IV, and C IV observed using the *Hopkins Ultraviolet Telescope (HUT)* requires multiple zones with differing column densities and ionization parameters (Kriss et al. 1996a). Likewise, multiple components with differing physical conditions are present in the X-ray spectrum (Kriss et al. 1996b). This inferred complexity is born out by the detection of four distinct kinematic components in high-resolution spectra of the C IV region using the *Goddard High Resolution Spectrograph (GHRS)* on the *Hubble Space Telescope (HST)* (Crenshaw, Maran, & Mushotzky 1998).

With observations of only one ion in the GHRS spectrum it is impossible to determine physical conditions in the absorbing gas. However, given the low velocities and widths of two of the C IV components, Crenshaw et al. (1998) suggest that they arise in gas in the interstellar medium or galactic halo of NGC 3516. They associate the more blue-shifted components with outflowing gas from the nuclear region. Given these characteristics, we planned *Far Ultraviolet Spectroscopic Explorer (FUSE)* observations of the 900–1200 Å spectrum of NGC 3516 to make high-resolution measurements of the O VI and Lyman-line absorption components. As shown by Kriss et al. (2000) for the Seyfert 1 Mrk 509, such observations can determine physical conditions in individual kinematic components of the UV-absorbing gas and detect which, if any, of them might be directly associated with the X-ray absorbing gas. Ascertaining the physical conditions of the individual components could give insight into the mechanisms giving rise to the outflow and hence to the origin of associated UV absorbers in Seyfert nuclei.

For NGC 3516, determining this structure could prove even more enlightening since it is one of the rare Seyfert 1s whose narrow-line region shows a bipolar morphology in the distribution of ionized gas around the nucleus (e.g., Pogge 1989; Aoki et al 1994; Ferruit, Wilson, & Mulchaey 1998). In addition, NGC 3516 has an opaque intrinsic Lyman limit (Kriss et al. 1996a), a feature seen only in the Seyfert 2 NGC 1068 and in only two other Seyfert 1s with a clear bipolar narrow emission line morphology: NGC 4151 and NGC 3227 (Kriss et al. 1997). In the scheme of unified models for Seyfert galaxies, this is unexpected. The standard model places the central engine and broad-line region in the interior of an opaque torus (see the review by Antonucci 1993). Light from the interior is collimated by the shadowing torus, and it illuminates the surrounding narrow-line region with a biconical pattern. Views from the pole of the torus give a full view of the interior, corresponding to an object we see as a Seyfert 1. Views in the plane of the torus show an obscured nucleus dominated by narrow-line emission exterior to the torus, corresponding to a Seyfert 2. Thus, both NGC 3516 and NGC 4151 appear spectroscopically as Seyfert 1s, but their narrow-line

morphology resembles that of Seyfert 2s. This suggests that we are viewing the interior close to the edge of the collimated pattern, as noted by Hutchings et al. (1998). Thus, the outflowing gas we see may be associated with the more opaque material responsible for collimating the ionizing radiation, or with an off-axis view of the central engine.

In this paper we describe FUSE observations of NGC 3516 in the 900–1200 Å spectral range and contemporaneous HST observations at longer UV wavelengths (1150 – 3100 Å) using the *Space Telescope Imaging Spectrograph (STIS)* that shed new light on the outflow phenomenon in Seyfert galaxies.

2. Observations

FUSE was designed to obtain high-resolution (R∼20,000) far-UV spectra covering the 905–1187 Å spectral range (Moos et al. 2000; Sahnow et al. 2000). Data are obtained in four independent optical channels, of which two use LiF coatings on the optics, and two use SiC. Two micro-channel plate detectors record individual photon events. A summary of the early FUSE observations of AGN is given by Kriss (2000). We observed NGC 3516 with FUSE on 2000 April 17, and with STIS (gratings G230L and G140L) on 2000 April 20. A full description of STIS and its performance are given by Kimble et al. (1998). As the AGN was in an unusually low state, the near-simultaneity of these observations was of importance (and by design). We thus have a good set of UV line profiles in the low state to compare with the normal high state observed earlier (Kriss et al. 1996a; Crenshaw et al. 1998; Goad et al. 1999).

The FUSE data were obtained in 11 consecutive orbits through the $30'' \times 30''$ apertures for a total exposure time of 16,382 s. As described by Sahnow et al. (2000), the data were processed using the standard FUSE pipeline to produce calibrated, one-dimensional spectra in each of the four channels. There were two exceptions to this process: first, we restricted the pulse heights of acceptable data to channels 4–16 to reduce the background; second, we measured the background in blank regions of each detector segment and scaled the background constant to this value. These steps improved the data quality on these faint exposures where the continuum flux of NGC 3516 is only about 1×10^{-14} erg s^{-1} cm^{-2} Å^{-1}. Since the LiF1 optical channel is also the one used by the fine guidance system on FUSE to maintain a precise pointing, the photometric stability of the LiF1 data is assured. In the other optical channels, thermal drifts can cause mis-centering of the target, leading to loss of flux and wavelength-scale errors. We therefore cross-correlated data from the other 3 channels with the overlapping wavelength range of the LiF1 channel to adjust their wavelength scales. We also applied gray-scale corrections to their flux levels to bring them

up to the same value as seen in the LiF1 spectrum. To achieve a workable signal-to-noise ratio (S/N) while maintaining enough resolution to recognize and remove H_2 absorption lines, the spectra were binned to a resolution of ∼0.5 Å. As the different FUSE channels have different S/N levels and residual scattered light problems, we assembled a complete 905–1187 Å spectrum by selecting the best data for each wavelength from among the four channels.

The STIS data were obtained in slitless mode. The G140L spectrum, covering the 1150–1700 Å wavelength range with a resolution of ∼ 1000, was obtained from a 600 s exposure. The G230L spectrum, covering the 1650–3100 Å range, was obtained in a 300 s exposure in the same orbit. No extended UV emission from the nuclear region of NGC 3516 was visible in our images. As the zero point of the wavelength calibration in slitless mode depends on the location of the target in the field of view, we extracted the one-dimensional STIS spectra in an iterative process. Using the STIS calibration pipeline in the Space Telescope Data Analysis System (STSDAS) `stis` package, we first obtained a preliminary spectrum. We measured the wavelengths of foreground Galactic absorption features, and used these to determine appropriate offsets for the centering of the target. We edited these offsets into the headers of the two-dimensional flat-fielded data frames (as is usually done by the wavelength calibration process in the pipeline) and re-ran the data through the pipeline to obtain our final calibrated spectra with corrected wavelength scales. Compared to the FUSE spectra, the STIS spectra are extracted from a much smaller angular region surrounding the nucleus. They have somewhat worse resolution but higher S/N. In the overlap region from 1150 to 1180 Å, the FUSE and STIS continuum levels match quite well, so it appears that the continuum arises almost entirely in the nuclear region with little to no contribution from starlight at larger radii in the FUSE aperture.

The diagrams illustrate the main features in the new spectra. We also compare our new spectra with data of lower resolution from HUT, which observed NGC 3516 in a high state in 1996 (Kriss et al. 1996a). For comparison of the whole FUSE wavelength range, the FUSE data were further smoothed to match the HUT data. As the overall FUSE signal level was low (due to the target faintness and observing time available), it was not possible to obtain detailed spectra of the Lyman lines and Lyman limit in NGC 3516. Therefore, the analysis and discussion below are not as detailed as would be warranted by better S/N data.

3. Line profile changes with nuclear flux changes

Figure 1 shows plots of lines from our data compared with earlier, high state, data. For easier comparison, the plots shown were placed on a velocity scale, centred at the galaxy redshift for each line. This is intended only to show the extent of the line asymmetries, which is not very sensitive to the range of uncertainty in the true redshift value. The 1996 data were also scaled to match the 2000 low-state continuum, for better comparison of the line profiles. This scaling is simply a factor applied to the entire flux so that the continuum levels beyond the emission lines match to within about 10%.

The O VI velocities are given with respect to redshift 0.0091. This is higher than the published value of 0.008836 and is derived from the reflection in velocity space that achieves the most symmetrical outer broad emission profile for O VI. The other lines shown used the published redshift value but were sufficently asymmetrical for various reasons that they were not useful for defining the redshift. There is uncertainty in this approach for O VI and the velocities in its plot are thus uncertain by some 50 km s^{-1}. The ubiquity of the shortward absorption in O VI, Lyα, and C IV in this current low state of the galaxy, and the strong narrow absorptions in all states, makes it hard to define the line centre precisely.

The top left FUSE O VI profile in Figure 1 is the combination of both O VI lines, after approximate removal of the H_2 absorptions, which were recognised from FUSE data of different targets with high S/N spectra. The plot at lower right shows both profiles without H_2 removal. The lower right plot also shows the HUT data on the same flux scale. The doublet ratio of the O VI line peaks in 2000 is nearer to unity than in the HUT 1996 data, indicating that the optical depth was greater in 2000.

The dashed lines on the left of the profiles are the reflected longward profile assuming the above velocity zero. They thus show the extent of the implied absorption in the profiles. The HUT Lyα profile is heavily contaminated by local absorption (and geocoronal emission) to its shortward side beyond -1000 km s^{-1} or so.

The FUSE and STIS data are essentially simultaneous (obtained on April 17 and 20, respectively). For comparison, the dotted profiles are the HUT data from 1996, when the nucleus was in a higher state. For easier profile comparison, the HUT data have been roughly scaled to match the 2000 continuum levels. Thus, the flux scale shown applies only to the year 2000 FUSE and STIS data. The changes in the relative absorption between 1996 and 2000 are clear from these comparisons. Note that the C IV absorptions seen earlier are still present, but that there is extra absorption at shorter wavelengths in the 2000 low state.

The upper right profiles show the broader Mg II and C III] profiles (the latter blended on its shortward side by Si III] 1892Å). As noted by Goad et al. (1999), these lines show

no changes or absorption from high to low state. The comparison between C IV and Mg II in centre right shows that the C IV broad emission profile matches the Mg II, with the absorptions lying below this broader profile.

Figures 2 and 3 show the full wavelength ranges of FUSE and the FUV channel of STIS, where other lines can be compared between the high and low states of NGC 3516. Similar changes are seen in Si IV, while the weaker line changes are more noisy. The large change in He II $\lambda 1640$ is probably due to the larger aperture in the HUT data including hot stars as well as the active nucleus. The Lyman absorptions seen in the HUT spectrum are not seen in the low-state FUSE spectrum. However, there is severe airglow contamination in Lyβ, and the signal is noisy and weak at the higher Lyman lines.

4. Low state line profiles

The broad line profiles (both emission and absorption) in the new low-state data strongly suggest that they are dominated by outflow at velocities not seen in the high state. The absorption and line width in O VI indicate outflow velocities of some 600 km s^{-1} in the hottest (highest ionisation) regions, with the bulk at about 400 km s^{-1}. There is absorption (outflow gas) at all velocities down to zero. The C IV and Lα profiles show the same velocity of maximum absorption and absorption to zero velocity, but the outflow occurs to higher velocity, with a second minimum at 1600 km s^{-1} and a terminal velocity of 2000 km s^{-1}. Much, but not all, of the low-velocity outflow is also present in the high-state profiles, and we know that these can be resolved into several sharp components, from higher resolution data from HST.

The lower resolution of the STIS spectra means that we cannot easily see whether there are sharp components to any of the current outflows. The HUT data on O VI have very poor resolution and noise but suggest a different O VI optical depth overall. We also see that the emission from the low ionisation and low density gas (C III] and Mg II) are the same as in the high state. Thus, we seem to be seeing a change in the state of the high-ionisation gas. As it coincides with continuum flux decrease, we speculate that there is increased absorption in the inner part of the BLR responsible for the overall phenomenon.

The scenario that we suggest for the broad emission and broad absorption features is of an accelerating wind like a stellar wind. The velocity increases and the ionisation decreases outwards. As the central source flux drops, the ionisation boundaries move inwards. Wide profiles with weak or non-detectable P-Cygni absorptions arise if lines are formed in a large radius region at terminal velocity. This is the situation in the high state (assuming the

narrow low velocity absorptions arise in places that lie far outside the wind region). In the low state, the high ionisation lines are formed at much smaller radii from the nucleus, where P-Cygni absorptions are more prominent, and can be seen through the whole absorbing column to the continuum source. The highest ionisation lines are narrower and have lower velocity absorptions. We describe and quantify this scenario in a little more detail in the next section.

We note that the C IV profile also contains strong low velocity absorption, in both high and low states. This is resolved in higher resolution HST data into several narrow features that do not change, and are similar to narrow absorptions seen in other Seyferts (Crenshaw et al. 1999). These arise in the general ISM and stable outflows that lie well outside the BLR (as seen also in NGC 4151 by Kaiser et al. 2000), and thus need to be ignored or our discussion of the BLR profiles. The FUSE resolution is high enough to show that the P Cygni absorption seen in O VI is not made of narrow features, but is broad, as expected from the wind model.

We note that the two higher velocity C IV absorptions resolved in high resolution HST spectra have velocities that are close to those seen in the FUSE O VI profiles. While the O VI profiles are not resolved into the distinct components seen in C IV, it is possible that the absorbing material is the same if the O VI absorbers are much more saturated. If this is so, then we require a different explanation in terms of variable high ionisation of dense material outside the BLR. It does not explain the narrowness of the O VI emission in the FUSE data. Thus, while acknowledging the possibility that the lower velocity absorbers have a different origin, we will discuss in more detail the disk wind idea that appears to explain more of the observed behaviour.

5. The wind scenario for the BLR

The profiles are broadly consistent with an accelerating wind, as present in OB stars. It is worth checking this idea for consistency, since it implies a very specific model for the BLR. Figure 4 outlines the scenario in cartoon fashion. The ionised gas that constitutes the BLR is accelerated away from the central continuum source until it approaches a terminal velocity. The terminal velocity is indicated by the overall width of the emission lines, and where there are P-Cygni absorptions, by the maximum blue-shifted absorption. There is an ionisation (temperature) gradient outwards from the central source. Line profiles are formed in the range of radius (hence velocity) where its ion is found. Thus, lines are formed in shells of increasing radius (and velocity) as the ionisation state decreases.

The cartoon profiles show qualitatively how the profiles differ as the shell of formation moves outward. These hold if the shells lie within a few times the radius of the continuum source. Thus, the absorption column is a decreasing fraction of the projected emission line region, as the shell radius increases. Close to the continuum source, there is strong absorption, and all velocities are low, so that the overall profile is narrow. It is also relatively 'peaky'. For shells of increasing radius, the overall profile width increases, and the absorption becomes weaker and occurs only at the shortward edge of the profile. Once terminal velocity is reached, the profile width remains the same, and the absorption becomes negligible at larger radii. The details of the profiles depend on the exact relationship between ionisation, radius, and velocity.

We note that this simple model is for spherically symmetric expansion, as expected for a star. If the wind is driven by a disk, the geometry becomes a further parameter, and the absorption and emission components may be separated if the rotation velocity is comparable to the outflow velocity. Knigge and Drew (1996) discuss disk winds seen in cataclysmic binary systems, that show some of these effects. Disk winds may be driven over a broad angle on each side of the disk, but not near the disk plane. Since AGN jets are also driven perpendicular to the disk, there may be a cone of wind avoidance where the jet lies, if there is one. The Seyfert 1 paradigm is that we view the central disk and BLR directly without obscuration by the opaque torus, and thus within the expected sightline of a central wind. The wind profiles for such a disk sightline are similar to those for a spherical wind, with slightly less peaky emission profiles. Thus, the simple wind cartoon is generally applicable to the expected geometry, but dependent in detail on the solid angle filled by the wind.

We note that the disk wind model of Murray et al. (1995) for BALQSOs blows close to the disk plane for objects of higher luminosity and outflow velocity (see also Elvis 2000). The hydromagnetic wind of Königl and Kartje (1994), on the other hand, is more collimated normal to the disk plane. Proga, Stone, and Kallman (2000) discuss the dynamics for disk winds from more massive central objects, and note the role of X-ray shielding and ionisation that launch and accelerate the wind in such models. The strong X-ray flux from the nuclear source is likely to highly ionize unshielded portions of the disk wind, as emphasized by Murray et al. (1995). This highly ionized portion of the wind could be associated with the X-ray warm absorber. Mathur et al. (1997) discuss X-ray warm absorbers in NGC 3516 in the context of an outflowing wind, but, unfortunately, we do not have contemporaneous X-ray spectra that would permit us to test their predictions.

We now postulate that the change between high and low states of NGC 3516 are principally expansion or shrinking of the ionisation radii within the wind, as shown in

the sketch. This would arise from changes in the amount of ionising radiation that are effectively the observed high and low luminosity states of the nucleus. The changes seen in the profiles of high, intermediate, and low ionisation, as illustrated by O VI, C IV, and Mg II, are much as observed. The postulated stratification is both a function of ionisation state as well as the line formation mechanisms in the wind. Both thermal emission and scattering contribute to the formation of wind emission lines. As in OB stars, the low-ionization lines are likely dominated by thermal emission, while scattering will dominate the observed high-ionization line emission. Since scattered line profiles are sensitive to the velocity gradient, broader lines are formed are larger radii. Thus, the overall idea seems feasible, *provided that the BLR lies within a few disk radii of the continuum source.*

We can also imagine that the high to low state changes involve changes in the continuum source radius or the velocity profile within the BLR. The flux changes are no more than a factor of 2–3, so that we do not expect disk-size or wind-acceleration changes to be large or rapid. The change of the ionisation radii will be the immediate and dominant effect in any case.

We can make a rough estimate of the radii, based on the assumption of similarity with OB stellar winds. The stellar winds are driven by the radiation pressure in the rest-frame UV where the strong absorptions lie that drive the wind by photon scattering. The nucleus of NGC 3516 has similar colour to an OB star, so we may compare the magnitudes to estimate the radiation that drives the winds. NGC 3516 has a redshift of $\sim$2650 km s^{-1} which gives it a distance of some 40 Mpc or distance modulus of about 33. The galaxy V magnitude is 12.4, (with the nucleus at 14 - 16) which yields an absolute magnitude of -20.6, of which the nucleus accounts for about -18. An OB star with a strong wind has absolute V magnitude of -7 (with similar colours), so that the nuclear continuum source is equivalent to some 60,000 OB stars. Assuming we require the same radiation level for the disk wind of NGC 3516, this implies a continuum source radius of 250 times that of an OB star, which is about 60 a.u. The BLR then should have a radius of several times this, which is about 2 light days in radius. Echo mapping observations indicate BLR diameters of a few light days for Seyferts. In the case of NGC 3516 it is measured at 4.5 days for the total C IV emission line flux (Koratkar et al 1996). Thus, within the uncertainties of the luminosity estimate above, the scenario seems very consistent with a radiation-driven wind for the BLR. In fact, the numbers above would *require* a wind to be present by the same processes that we understand for stellar winds.

It is interesting to see how the masses and mass flows scale in this rough comparison. Stellar winds have terminal velocities closely related to the surface escape velocity of the star. The terminal velocity in NGC 3516 is $\sim$2000 km s^{-1}, very typical of stellar winds,

so that if the mechanisms are the same, the average effective gravity at the base of the AGN wind should be comparable with an OB star. The average particle at the surface of the AGN accretion disk (of radius 250 OB star radii) lies at distance $\sim$200 OB star radii from the central object. To make the gravity equal in both cases requires a central mass of about 10^6 $M_\odot$, which again is the right order of magnitude. If we scale the mass loss against typical stellar winds of about 10^{-6} $M_\odot$ per year, allowing that the AGN wind may fill say 1/4 of a sphere, we find a mass-loss rate of a few $M_\odot$ per year. This again is not unreasonable, but would be significant in the accretion budget for the AGN.

In in more comprehensive picture, we note that ionisation by high energy photons from the AGN will alter the wind as its opacity changes with height, probably giving rise to the warm absorbers seen in the X-ray spectra. The wind structure that may apply in NGC 3516 will need detailed modelling, and comparison with data from different luminosity states will help define the important ionisation structure. Such modelling—particularly the dynamics of rotation and acceleration of the wind— must await more and better contemporaneous data at FUV and X-ray wavelengths.

Our principal conclusion from the present data is that we feel there is significant evidence that the BLR in NGC 3516 is an accelerating wind driven by the nuclear continuum source, that is seen in sightlines within the cone of UV ionisation. If this applies in a more general way, we might expect to see similar profile changes in other Seyferts with very low states. In the case of NGC 4151, this does seem to be true: P Cygni profiles are seen in lines in low states - most notably in data taken in the current (year 2000) low state by STIS. We therefore suggest that careful monitoring of line profiles with nuclear flux would be a valuable way of verifying the model proposed and learning more about how it works.

Our discussion relates to the connection between broad-line profile widths and the mass of the central black hole. Clearly, any motions in the central region are dominated by the gravitational field, whether they be in Keplerian orbit, free-falling, moving with escape velocity, or driven by radiative forces. More detailed wind models may enable us to use profile widths to test them, and thereby formulate the relation between observed profiles and central mass. We note that the low state of NGC 3516 we have sampled, may reveal the inner part of the outflow not often seen in more luminous and extended BLRs, where line widths are no longer radiatively driven.

Finally, we note that the highest ionisation lines, such as the Fe K line seen at 7Kev in X-ray spectra, have profiles that show they arise in a disk of relativistic velocities, so do not arise in the BLR wind, but in the continuum source disk itself (Nandra et al. 1999).

6. Other spectral features

Figure 2 shows the entire FUSE range spectrum compared with the same range with HUT in 1996. For this plot, the FUSE data were selected to use only the best data for each wavelength region, and then smoothed to about 0.4 Å resolution, for easier comparison of the broad weak features. The airglow lines have been removed, but not the H_2 absorptions, which must be present in both datasets. The HUT data also show zero redshift Lβ absorption which has not been removed. At the shortest wavelengths, there are probably detector and noise effects that are not real differences.

The lines present other than O VI are N III λ990, He II λ1085, and possibly N IV λ948 and S IV+Si IV λ1063-66. The C III λ977 line is not detectable, while the other lines are all narrower as well as weaker than in the 1996 spectrum. There are very broad features that appear to be associated with the lines of C III, N III, O VI, and He II that are seen at both epochs, for which we offer no detailed explanation. The overall continuum level in 2000 is about 1/3 that of 1996, and the broad features all scale with this same factor. There are differences at the positions of N III and the S IV/Si IV blend. Sharper emissions are seen on top of the broad wings at He II (only in 2000) and N III and O VI.

Moving to longer wavelengths (1200 to 1800 Å), Figure 3 shows the comparison between the 1996 HUT data and the 2000 STIS data. The flux level difference becomes smaller with increasing wavelength and is close to 2 at 1800 Å. Aside from emission line profile changes, the relative strength of He II and N III] are lower in the 2000 low state. Since it is unlikely that the forbidden line flux changes significantly, the difference is probably due to the line emission arising over an extended region that is differently sampled by the STIS and HUT slits. The FUSE and STIS continuum levels match quite well where they join, so that it appears that the continuum arises almost entirely in the nuclear region. The drop in He II λ1640 flux between HUT and STIS may also indicate an extended origin of this emission, since the He II λ1085 line does not show the same drop in flux. He II λ1640, along with He II λ4686, arises in hot stars and thus may well be extended in this galaxy. Thus, among the weaker emission lines from the nuclear region, both N III and He II have developed sharp components in the 2000 low state.

7. Discussion

The paradigm of the unified model for AGN is that in Seyfert 1 galaxies, we view the broad line region from within the cone of light illuminated by the nucleus. The cone is caused by shadowing of an equatorial region by an opaque torus around the nucleus:

Seyfert 2s are those nuclei hidden by the torus. Inside the cone there is ionising radiation, radio jet material, and clouds of narrow emission line material. Recent data from STIS (e.g. Hutchings et al. 1998, Kaiser et al. 2000, Crenshaw et al. 2000) suggest that the narrow-line material is moving outwards at a few hundred km s^{-1} along the inside surfaces of the cones, and not filling them. The STIS data indicate there are also faster moving clouds that fill a wider angle and arise close to the nucleus (Hutchings et al. 1999). These are seen both in absorption and emission, and the former are usually stable over years. Occasionally some narrow absorptions change or new ones appear.

In addition to these narrow and relatively stable absorbers, the change of broad line profiles from 1996 to 2000 suggest that they may be explained by an outflowing BLR. This paper has explored the way in which the change of state allows us to probe the velocity structure of a broad-line wind, by varying the radii of the shells in which different lines are formed. We think that the density structure may not change significantly. The geometry of the wind, what happens to its material as it moves outward and cools, and its relationship with the other mass flows, need to be considered and tested with observations in other objects as well as NGC 3516 itself as it continues to vary. Our scenario predicts a close link between the BLR profiles and the continuum flux, which can be done with continued monitoring, particularly in the O VI lines.

Kriss et al. (1996a) note that the presence of Lyman limit absorption and the S-shaped NLR in NGC 3516 may imply a line of sight near to the edge of the cone, as in NGC 4151. This does not preclude the disk wind scenario, but it would be useful to study the NLR dynamics in detail for more geometrical clues, and obtain better FUSE data to look for the Lyman absorption lines and limit.

There have been other discussions of the BLR of NGC 3516, based on monitoring campaigns for echo-mapping, as well as more sporadic observations of high and low states and the occasional presence of BAL-type absorption (e.g. Wanders et al 1993, Koratkar et al 1996, Goad et al 1999). The suggested model in this paper is consistent with these other discussions, none of which have proposed a detailed model.

NGC 3516 has a NLR component, which we assume does not change with the nuclear and BLR changes, since it is formed in the much more extended S-shaped region noted above. This component is not seen in the UV lines in Figure 1, although Goad et al (1999) model profiles with a narrow component of FWHM some 1200 km s^{-1}. The narrow emission peak seen in O VI is much narrower than this, and is unlikely to represent the NLR emission for this reason as well as for its high ionisation. Aoki et al (1994) also discuss the ionisation of the NLR and its relationship to the nuclear source.

Our FUSE profiles of O VI are key to our suggested model, and we have noted that a higher S/N would be very useful in checking whether these lines do contain NLR components such as the narrow absorbsions and emission peak. With the data in hand we favour the explanation that they arise in the inner accelerating part of a central mass flow.

There are some clues in other objects. VLBI radio maps of NGC 4151 shows a bend close to the nucleus (Roy et al. 1999), where the radio structure becomes aligned with the outer ionisation cones and radio structure. The same galaxy also shows P Cygni profiles occasionally, and notably in its current low state. In NGC 4151, our line of sight is deduced to be close to the edge of the cone.

The relation between line FWHM and reverberation time lag (Peterson and Wandel 2000) for other AGN, indicates that in those cases the line profiles become narrower with distances from the nucleus that are larger than those we consider here. This would indicate that the wind velocity falls again at radii where the radiation pressure has dropped and the wind material is slowed by interactions with the ambient medium. It is only in cases such as the low state of NGC 3516, that broad line formation is dominantly in the inner accelerating region.

We may further speculate whether a wind model for BLR applies to more energetic QSOs. These have lines (and BAL velocities) that are higher by a factor of several, luminosities higher by up to 100 or more, BLR sizes (from variability timescales) larger by about 100, and central masses probably 2 to 3 orders of magnitude higher. These numbers all scale quite reasonably to winds, although the above parameters are not tightly linked to each other. Good resolution and S/N studies of variations in highly ionised emission lines in a range of AGN will be necessary to pursue these questions.

This work is based on data obtained for the Guaranteed Time Team by the NASA-CNES-CSA FUSE mission operated by the Johns Hopkins University. Financial support to U. S. participants has been provided by NASA contract NAS5-32985.

REFERENCES

Antonucci, R.R.J. 1993, ARA&A, 31, 473

Aoki, K., Ohtani, H., Yoshida, M., & Kosugi, G. 1994, PASJ, 46, 539

Crenshaw, D. M., Maran, S. P., & Mushotzky, R. F. 1998, ApJ, 496, 797

Crenshaw D.M., Kraemer S.B., Boggess A., Maran S.P., Mushotzky R.F., Wu C-C, 1999, ApJ, 516, 750

Crenshaw D.M. et al. 2000, in press (astro-ph 0007017)

Elvis M. 2000, ApJ, 545, 63

Ferruit, P., Wilson, A. S., & Mulchaey, J. S. 1998, ApJ, 509, 646

George, I. M., et al. 1998, ApJS, 114, 73

Goad M.R., Koratkar A.P., Axon D.J., Korista K.T., O'Brien P.T., 1999, ApJ, 524, 707

Hutchings, J.B., et al. 1998, ApJ, 492, L115

Hutchings, J.B., et al. 1999, AJ, 118, 2101

Kaiser, M.E., et al. 2000, ApJ, 528, 260

Kimble, R., et al. 1998, ApJ, 492, L83

Königl, A., & Kartje, J. F. 1994, ApJ, 434, 446

Koratkar, A. P., et al. 1996, ApJ, 470, 378

Knigge C., and Drew J.E., 1996, MNRAS, 281, 1352

Kriss G. A., et al. 1996a, ApJ, 467, 622

Kriss G.A. Espey B.R., Krolik J.H., Tsvetanov Z., Zheng W., Davidsen A.F., 1996b, ApJ, 467, 629

Kriss, G. A., et al. 1997, in ASP Conf. Ser. Vol. 113, Emission Lines in Active Galaxies: New Methods and Techniques, eds. B.M. Peterson, F.-Z. Cheng, & A.S. Wilson (San Francisco: ASP), 453

Kriss, G. A., et al. 2000b, ApJ, 538, L17

Kriss, G.A. 2000, to appear in the proceedings of the workshop on “Probing the Physics of Active Galactic Nuclei by Multiwavelength Monitoring, eds. B. Peterson, R. Polidan, & R. Pogge, (ASP:San Franciso), in press (astro-ph 0008492)

Mathur, S., Wilkes, B., & Elvis, M. 1995, ApJ, 452, 230

Mathur, S., Wilkes, B., Elvis, M., & Fiore, F. 1994, ApJ, 434, 493

Mathur, S., Wilkes, B., & Aldcroft, T. 1997, ApJ, 478, 182

Moos et al. 2000, ApJ, 538, L1

Murray, N., Chiang, J., Grossman, S. A., Voigt, G. M. 1995, ApJ, 451, 498

Nandra K., George I.M., Mushotzky R.F., Turner T.J., Yaqoob T., 1999, astro-ph 9907193

Peterson B. M., & Wandel A., 2000, in press (astro-ph 0007147)

Pogge, R. 1989, AJ, 98, 124

Proga D., Stone J.M., Kallman T.R., 2000, ApJ, 543, 686

Reynolds, C. S. 1997, MNRAS, 286, 513

Roy, A.L., Ulvestad, J.S., Colbert, E.J.M., Wilson, A.S, & Norris, R.P. 1997, IAU Colloq 164

Sahnow D., et al. 2000, ApJ, 538, L7

Ulrich, M.-H. 1988, MNRAS, 230, 121

Wanders I, et al. 1993, A&A, 269, 39

Weymann, R. J., Morris, S. L., Foltz, C. B., & Hewett, P. C. 1991, ApJ, 373, 23

This preprint was prepared with the AAS LaTeX macros v4.0.

Figure captions

1. Comparison in velocity space with respect to the galaxy velocity, of profiles from 2000 low state with 1996 high state. In the left panels, the dashed lines show the reflected longward profile to highlight the shortward absorption. The top left O VI profile combines both lines of the doublet, with the H_2 absorptions removed. The full O VI data are shown in lower right panel, with H_2 lines marked with vertical dashes. The 1996 fluxes have been scaled to match the continuum levels from the low state, to show the profile differences. FUSE data are smoothed to 0.5 Å resolution and the HUT data have 2 Å resolution. Note the increased broad absorption in the low state data.

2. Comparison of the low and high state spectra over the entire FUSE range. The FUSE data are smoothed to match the HUT data, and the HUT data are displaced in Y by $2\text{x}10^{-14}$ (dashed line) for clarity. The principal broad emission lines are identified above the HUT spectrum. Other broad features with possible identifications are marked where they are seen in the FUSE data. In addition to the strong O VI, N III and He II emission peaks, there appear to be broad components that scale with the continuum. Overlapping STIS coverage is shown as dotted line.

3. Comparison of the STIS FUV spectral range with the HUT high state spectra. Note the profile changes in Si IV, and He II as well as those shown in Figure 1.

4. Sketch showing the way that a contraction of the ionisation structure in the low state can explain the profile changes seen. While no units are given, radii range from the surface of the continuum source to several times its radius. The text discusses this diagram in detail.

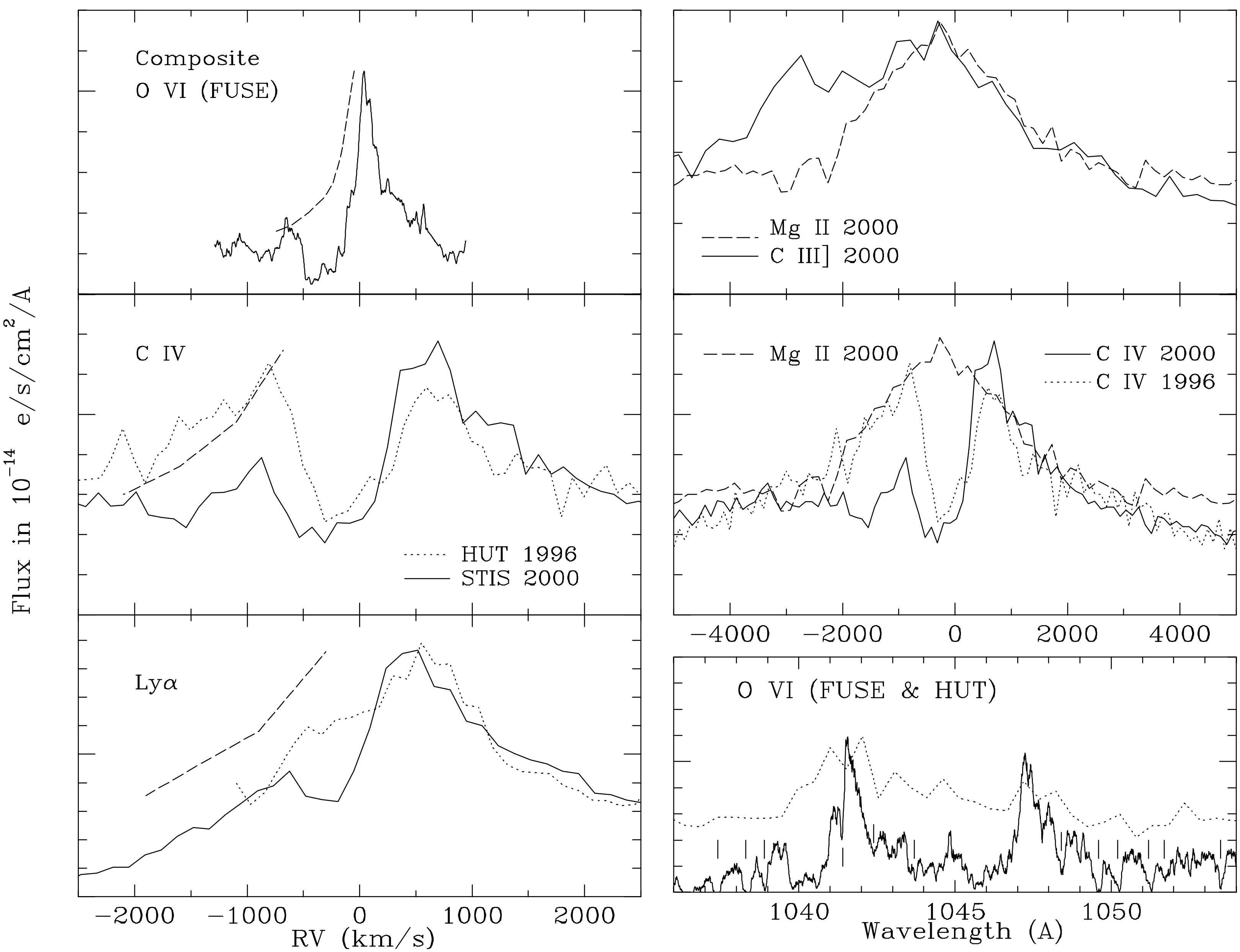
Flux in 10^{-14} e/s/cm^2/A
Composite
O VI (FUSE)
C IV
HUT 1996
STIS 2000
Lyα
RV (km/s)
Mg II 2000
C III] 2000
Mg II 2000
C IV 2000
C IV 1996
O VI (FUSE & HUT)
Wavelength (A)

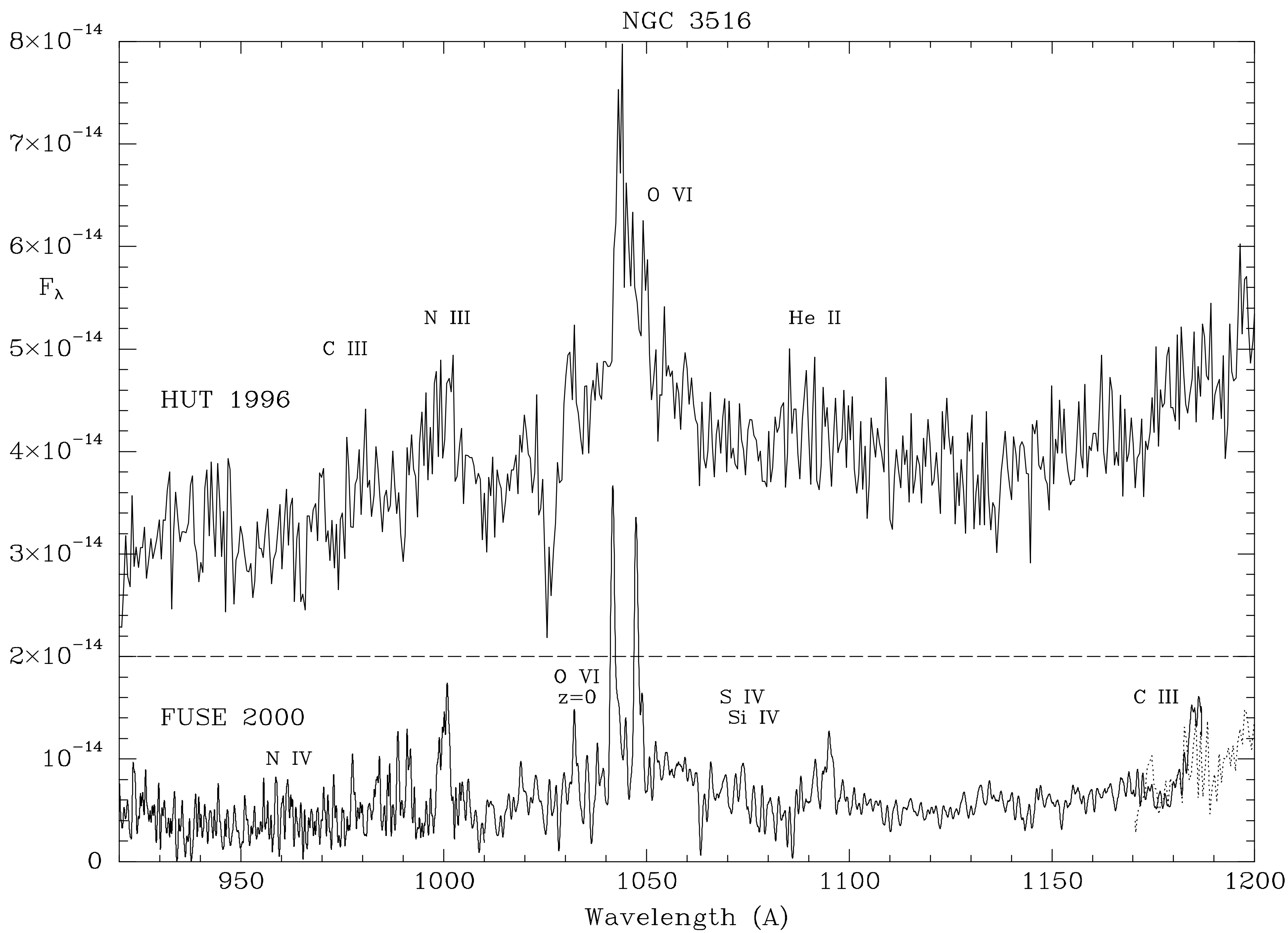
NGC 3516
HUT 1996
FUSE 2000
C III
N III
O VI
He II
N IV
O VI
z=0
S IV
Si IV
C III
F_λ
Wavelength (A)
8×10^{-14}
7×10^{-14}
6×10^{-14}
5×10^{-14}
4×10^{-14}
3×10^{-14}
2×10^{-14}
10^{-14}
0
950
1000
1050
1100
1150
1200

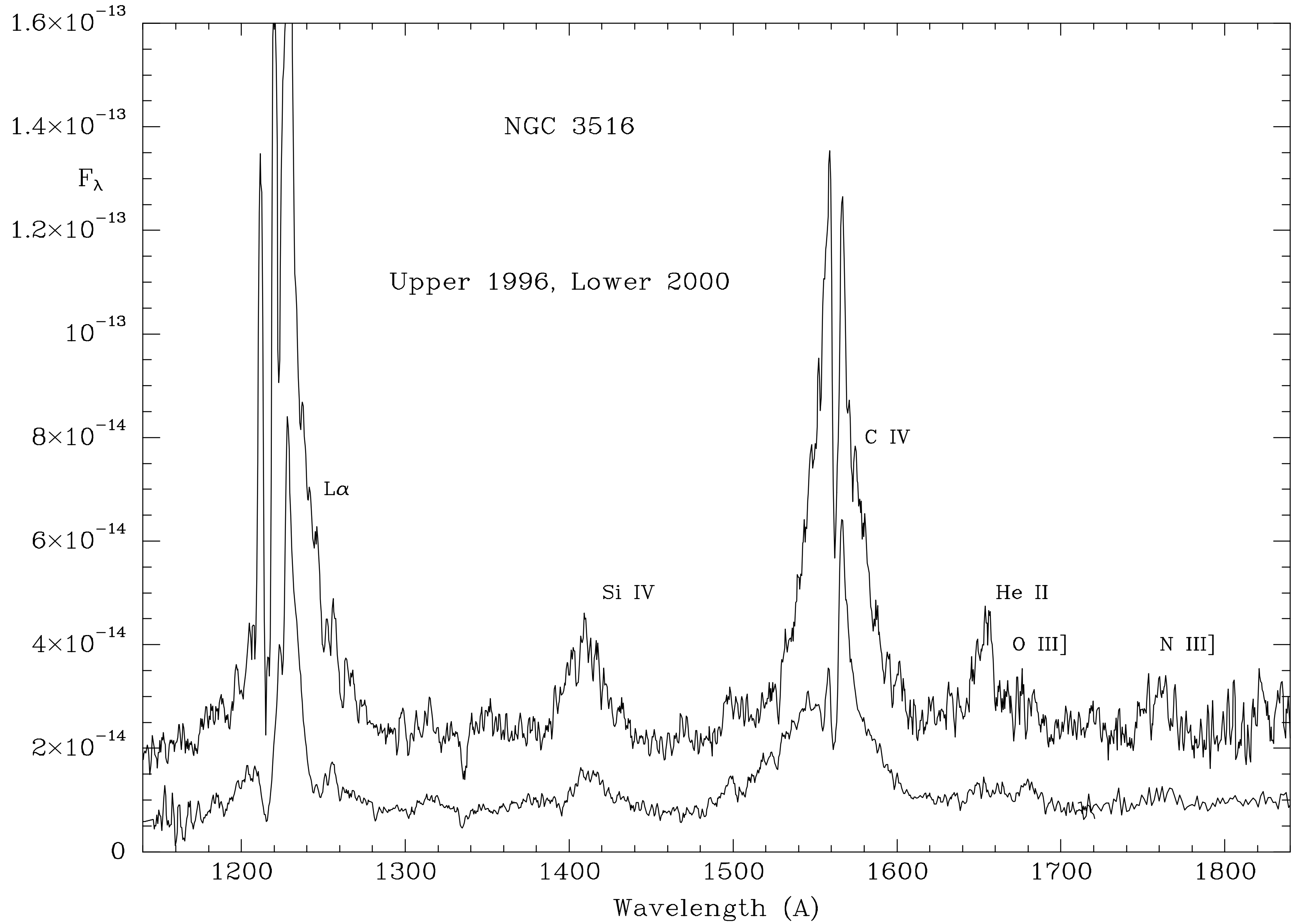
NGC 3516
Upper 1996, Lower 2000
F_λ
1.6×10^-13
1.4×10^-13
1.2×10^-13
10^-13
8×10^-14
6×10^-14
4×10^-14
2×10^-14
0
1200
1300
1400
1500
1600
1700
1800
Wavelength (A)
Lα
Si IV
C IV
He II
O III]
N III]

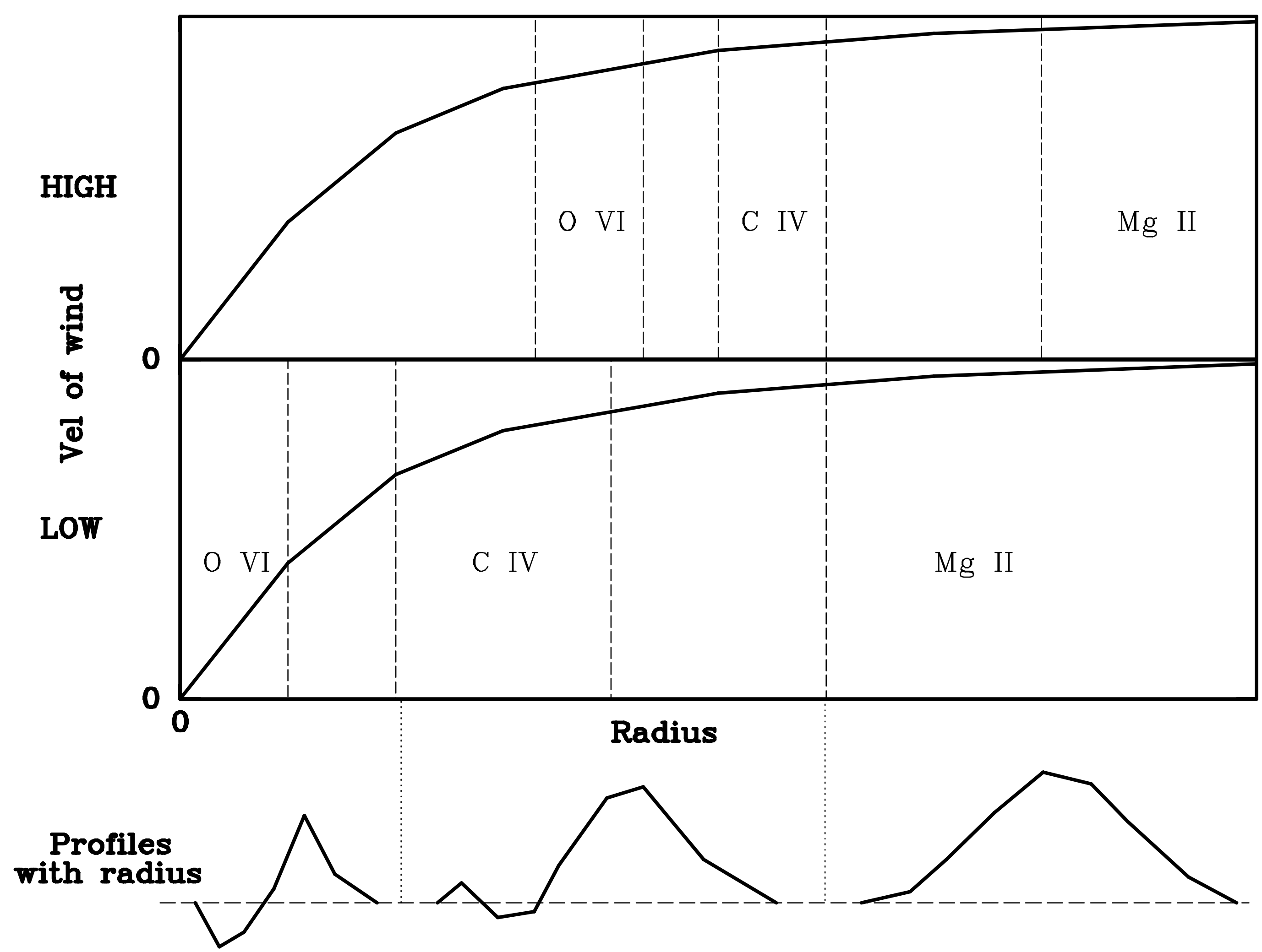
HIGH
O VI
C IV
Mg II
Vel of wind
0
LOW
O VI
C IV
Mg II
0
0
Radius
Profiles
with radius